Asymmetrical Distribution of Ca-Activated Cl Channels in *Xenopus* Oocytes

Khaled Machaca and H. Criss Hartzell

Department of Cell Biology, Emory University School of Medicine, Atlanta, Georgia 30322-3030 USA

ABSTRACT *Xenopus* oocytes are a popular model system for studying Ca signaling. They endogenously express two kinds of Ca-activated Cl currents, $I_{Cl\text{-}1}$ and $I_{Cl\text{-}2}$. $I_{Cl\text{-}1}$ is activated by Ca released from internal stores and, with appropriate voltage protocols, by Ca influx. In contrast, $I_{Cl\text{-}2}$ activation is dependent on Ca influx. We are interested in understanding how these two different Cl channels are activated differently by Ca from different sources. One could hypothesize that these channels are activated differently because they are differentially localized near the corresponding Ca source. As an initial investigation of this hypothesis, we examined the distribution of $I_{Cl\text{-}1}$ and $I_{Cl\text{-}2}$ channels in the oocyte. We conclude that both $I_{Cl\text{-}1}$ and $I_{Cl\text{-}2}$ channels are primarily localized to the animal hemisphere of the oocyte, but that capacitative Ca influx occurs over the entire oocyte membrane. Evidence supporting this view includes the following observations: 1) Injection of IP_3 into the animal hemisphere produced larger and faster $I_{Cl\text{-}1}$ responses than injection into the vegetal hemisphere. 2) Exposure of the animal hemisphere to Cl-free solution almost completely abolished $I_{Cl\text{-}1}$ produced by IP_3-induced release of Ca from internal stores or by capacitative Ca entry. 3) Loose macropatch recording showed that both $I_{Cl\text{-}1}$ and $I_{Cl\text{-}2}$ currents were approximately four times and approximately three times, respectively, more dense in the animal than in the vegetal hemisphere. 4) Confocal imaging of oocytes loaded with fluorescent Ca-sensitive dyes showed that the time course of activation of $I_{Cl\text{-}1}$ corresponded to the appearance of the wave of Ca release at the animal pole. 5) Ca release and Ca influx, although twofold higher in the animal pole, were evident over the entire oocyte.

INTRODUCTION

Xenopus oocytes are a popular model system for studying Ca signaling (DeLisle, 1991), because their large size facilitates visualization of Ca waves by using Ca-sensitive dyes (Lechleiter and Clapham, 1992; Camacho and Lechleiter, 1995; Parker et al., 1996; DeLisle and Welsh, 1992) and because they contain Ca-activated Cl channels that can be used as indicators of Ca concentration at the plasma membrane (Dascal, 1987; Parker and Miledi, 1987; Hartzell, 1996). We have recently reported that *Xenopus* oocytes contain two distinct species of Ca-activated Cl currents whose activation depends on the source of Ca (Hartzell, 1996; Hartzell et al., 1997). One Cl current ($I_{Cl\text{-}1}$) is activated as a result of Ca released from intracellular IP_3-sensitive Ca stores, whereas the other current ($I_{Cl\text{-}2}$) is activated by Ca influx from the extracellular space. These currents develop with different kinetics after intracellular injection of IP_3 and exhibit different biophysical characteristics (Hartzell, 1996). $I_{Cl\text{-}1}$ is activated immediately as injection of IP_3 stimulates Ca release from stores, but the current declines to baseline over the next few minutes as the stores become depleted of Ca. $I_{Cl\text{-}1}$ does not depend on extracellular Ca, has a linear instantaneous current-voltage relationship, and exhibits voltage-dependent activation at positive membrane potentials in the presence of Ca. As the stores become depleted of Ca and $I_{Cl\text{-}1}$ declines, capacitative Ca entry (Putney, 1990; Fasolato et al., 1994; Berridge, 1995; Clapham, 1995) becomes activated, and this Ca activates $I_{Cl\text{-}2}$. $I_{Cl\text{-}2}$ has a strongly outwardly rectifying instantaneous *I-V* curve and is activated at hyperpolarizing potentials that increase the driving force for Ca influx. $I_{Cl\text{-}2}$ is never activated by Ca released from stores. In contrast, $I_{Cl\text{-}1}$ can be activated transiently by Ca influx if the cell is first hyperpolarized to increase Ca influx and then depolarized to activate the voltage gate.

Our conclusion that these two currents are mediated by two different channels differs from previous interpretations. Parker and Yao (Parker and Yao, 1994; Yao and Parker, 1993) interpret their data in terms of a single population of Ca-activated Cl channels that exhibit different kinetic behaviors because the channels respond to the rate of change of the Ca signal and because the Ca signal exhibits complex spatial and temporal features resulting from feedback and feedforward interactions between influx and release (Girard and Clapham, 1993). Although it is possible that $I_{Cl\text{-}1}$ and $I_{Cl\text{-}2}$ are different manifestations of the same Cl channel caused by different Ca dynamics after Ca release from stores and capacitative Ca influx, this seems unlikely because $I_{Cl\text{-}1}$ and $I_{Cl\text{-}2}$ have different instantaneous current-voltage relationships (Hartzell, 1996). Because the instantaneous current-voltage relationship measures the current through open channels and is independent of channel gating, it is very difficult to imagine how these two currents can be explained in terms of a single channel, unless the temporal features of the Ca signal alter the ion permeation through the channel. Furthermore, the suggestion that the Ca-activated Cl channels respond to the rate of change of

Received for publication 27 June 1997 and in final form 9 December 1997.

Address reprint requests to Dr. H. Criss Hartzell, Department of Cell Biology, Emory University School of Medicine, 1648 Pierce Drive, Atlanta, GA 30322-3030. Tel.: 404-727-0444; Fax: 404-727-6256; E-mail: criss@cellbio.emory.edu.

0006-3495/98/03/1286/10 $2.00

the Ca concentration has recently been questioned by Gomez-Hernandez et al. (1997), who showed that the *Xenopus* Ca-activated Cl channels in excised inside-out macropatches respond to the steady-state Ca levels and not the rate of change of Ca concentration. For these reasons, we prefer the interpretation that these two currents are mediated by different channel populations. However, it is worth mentioning that there is no evidence at the single-channel level for two kinds of Ca-activated Cl channels.

The presence of two Ca-activated Cl channels in the oocyte that are activated differentially by Ca released from stores and Ca influx raises a number of interesting questions regarding the mechanisms by which the same chemical signal (in this case Ca) coming from different sources can regulate different effectors. The mechanisms could hypothetically involve differences in the spatial or temporal relationships between the Ca signals and the effectors, or could reflect differences in the concentration of Ca sensed by the two effectors when Ca comes from stores or influx (Thomas et al., 1996; Ghosh and Greenberg, 1995; Lenzi and Roberts, 1994; Quarmby and Hartzell, 1994). To answer these questions, it is important to know the relative distribution of Cl channels, Ca stores, and Ca influx channels in the oocyte. In this paper we have examined the distribution of $I_{Cl\text{-}1}$ and $I_{Cl\text{-}2}$ channels on the oocyte membrane in relationship to Ca release and influx. We conclude that capacitative Ca entry occurs over the entire oocyte surface, but that both $I_{Cl\text{-}1}$ and $I_{Cl\text{-}2}$ channels are mostly localized to the animal hemisphere.

EXPERIMENTAL PROCEDURES

Isolation of *Xenopus* oocytes

Stage V-VI oocytes were harvested from adult *Xenopus laevis* females (*Xenopus* I, Ann Arbor, MI) as described by Dascal (1987). *Xenopus* were anesthetized by immersion in Tricaine (1.5 g/liter). Ovarian follicles were removed, cut into small pieces, and digested in normal Ringer's with no added calcium, containing 2 mg/ml collagenase type IA (Sigma Chemical Co., St. Louis, MO), for 2 h at room temperature. The oocytes were extensively rinsed with normal Ringer's, placed in L-15 medium (Gibco BRL, Gaithersburg, MD), and stored at 18°C. Oocytes were used 1–6 days after isolation.

Imaging and electrophysiological methods

Xenopus oocytes were injected with 13.8 nl 70 kDa dextran coupled to Ca-Green-1 and Texas Red (Molecular Probes, Eugene, OR) for a final calculated intraoocyte concentration of ~22 μM Ca-green-1 and 13 μM Texas Red. Texas Red and Ca-Green-1 fluorophores were coupled to the same dextran molecule. Injected oocytes were voltage-clamped with two microelectrodes by the use of a GeneClamp 500 (Axon Instruments, Foster City, CA). Electrodes were filled with 3 M KCl and had resistances of 1–2 MΩ. The oocyte resting potentials were between −30 mV and −60 mV. Typically, the membrane was held at −35 mV, and stepped to +40 mV for 2 s and −140 mV for 2 s. Stimulation and data acquisition were controlled by Curcap32 (Software and hardware developed by Mr. Bill Goolsby, Emory University) via a Pentium 90 MHz PC. Images (256 × 256 pixels) were acquired 500 ms after the onset of each voltage pulse using a Zeiss LSM 410 confocal box fitted to an Axiovert 100 TV Zeiss inverted microscope with a Zeiss 10× objective (0.5 NA). The confocal aperture was set at the maximum opening, resulting in a focal section of 1270 × 1270 × 35 μm. Because Ca-Green-1 is a nonratiometric dye, the physically coupled non-calcium-sensitive Texas Red fluorescence was used to correct for dye distribution and quenching artifacts. Ca-Green-1 was excited with a 488-nm line from an argon laser, and Texas Red was excited with a 543-nm line from a helium neon laser. Image data were analyzed using the Zeiss LSM software and National Institutes of Health Image version 1.60. Current data were analyzed using Origin, version 4.1 (Microcal Software, Northampton, MA). Experiments were performed at room temperature (22–26°C). Normal pigmented oocytes were used for all experiments shown here. The pigment in the animal pole greatly attenuates the fluorescence signal, but the use of the Ca-green/Texas Red ratio permitted comparison between animal and vegetal poles. The same experiments have also been done on albino oocytes with identical results, except that there was usually some ambiguity about the orientation of animal/vegetal poles.

Two-sided perfusion chamber

The two-sided perfusion chamber is shown in Fig. 1. A conical hole was made in a thin sheet of plastic that separated two chambers that were separately superfused with solutions at 0.5 ml/min. The conical hole was made from a small section of a 200-μl pipette tip with an upper inside diameter of ~600 μm. This insert was carefully glued into a hole drilled into the partition. The inflow for the lower chamber was directed toward the oocyte to ensure rapid mixing of the solutions on the underside of the oocyte. The oocyte was placed in the hole and impaled with the voltage-clamping electrodes and the injection pipette to force the oocyte into the hole. In some experiments, the solution flowing into the lower chamber contained phenol red to permit visual evaluation of leakage of solutions around the oocyte. The upper and lower chambers joined at a point ~2 cm from the oocyte at the point where the perfusing solution was aspirated to waste.

Loose macropatch recording

The distribution of Cl channels on the oocyte membrane was also measured by using a large patch pipette attached to a List EPC-7 patch-clamp amplifier in current clamp mode. A glass micropipette was broken and fire-polished to an internal tip diameter of 40 μm. The pipette was positioned on the surface of an oocyte that was voltage-clamped with two microelectrodes. Negative pressure was applied to the macropipette to suck a small bleb of the oocyte into the tip of the pipette. The pipette could be repeatedly removed and repositioned. Multiple measurements of the same spot on the oocyte provided current amplitudes consistent within 20%. For these experiments, the bath potential was clamped at zero by a virtual

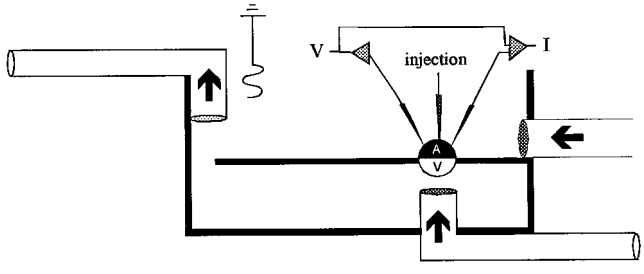

FIGURE 1 Two-sided perfusion chamber. The oocyte (A, animal hemisphere; V, vegetal hemisphere) is placed in a conical hole in a thin plastic sheet that separates two chambers that are independently perfused with solution at a rate of 0.5–2 ml/min. The oocyte is impaled with two microelectrodes for voltage clamp and an injection pipette for injecting IP_3. Both chambers are grounded by a 3 M KCl agar bridge positioned near the confluence of the two chambers and the outflow.

ground amplifier. When the macropatch pipette was moved away from the immediate surface of the oocyte, no potential change was recorded.

Oocyte injection

Oocytes were injected with IP_3 by using a Nanoject Automatic Oocyte Injector (Drummond Scientific Co., Broomall, PA). The injection pipette was pulled from glass capillary tubing in a manner similar to the preparation of the recording electrodes and then broken so that it had a beveled tip with an inside diameter of <20 μm. Typically, 23 nl of 1 mM IP_3 solution in Chelex-resin treated H_2O was injected to give a calculated oocyte concentration of $\sim$25 μM. The Ca concentration in this solution was not buffered, but injection of H_2O produced no change in Ca-Green fluorescence or membrane current.

Solutions

Normal Ringer's consisted of 123 mM NaCl, 2.5 mM KCl, 2 mM $CaCl_2$, 1.8 mM $MgCl_2$, 10 HEPES (pH 7.4). Zero Ca Ringer's was the same, except that $CaCl_2$ was omitted, $MgCl_2$ was increased to 5 mM, and 0.1 mM EGTA was added. Chloride-free solution was 123 mM Na-aspartate, 2.5 mM K-aspartate, 2 mM Ca-aspartate, 10 mM HEPES (pH 7.4). Stock solutions of IP_3 were made at 10 mM in H_2O, stored at -20°C, and diluted in water to the final concentrations indicated for injection. In all cases, injection of the same volume of water had no effect on the Cl currents.

RESULTS

Kinetics of $I_{Cl\text{-}1}$ activation

Initial experiments where we injected IP_3 into the animal or vegetal hemisphere suggested that Cl channels were asymmetrically distributed in the oocyte. We observed that the response to IP3 injection occurred more rapidly and was larger when IP_3 was injected into the animal pole (Fig. 2). In a typical oocyte injected in the animal hemisphere (Fig. 2 *A*, *closed squares*; Fig. 2 *B*), $I_{Cl\text{-}1}$ increased maximally to $\sim$5 μA within 10 s of injection. The current then decayed back to baseline in $\sim$2.5 min. In a different oocyte injected in the vegetal hemisphere (Fig. 2 *A*, *open circles*; Fig. 2 *C*), $I_{Cl\text{-}1}$ increased in two distinct phases. The first phase consisted of a small increase to 0.5 μA, which developed

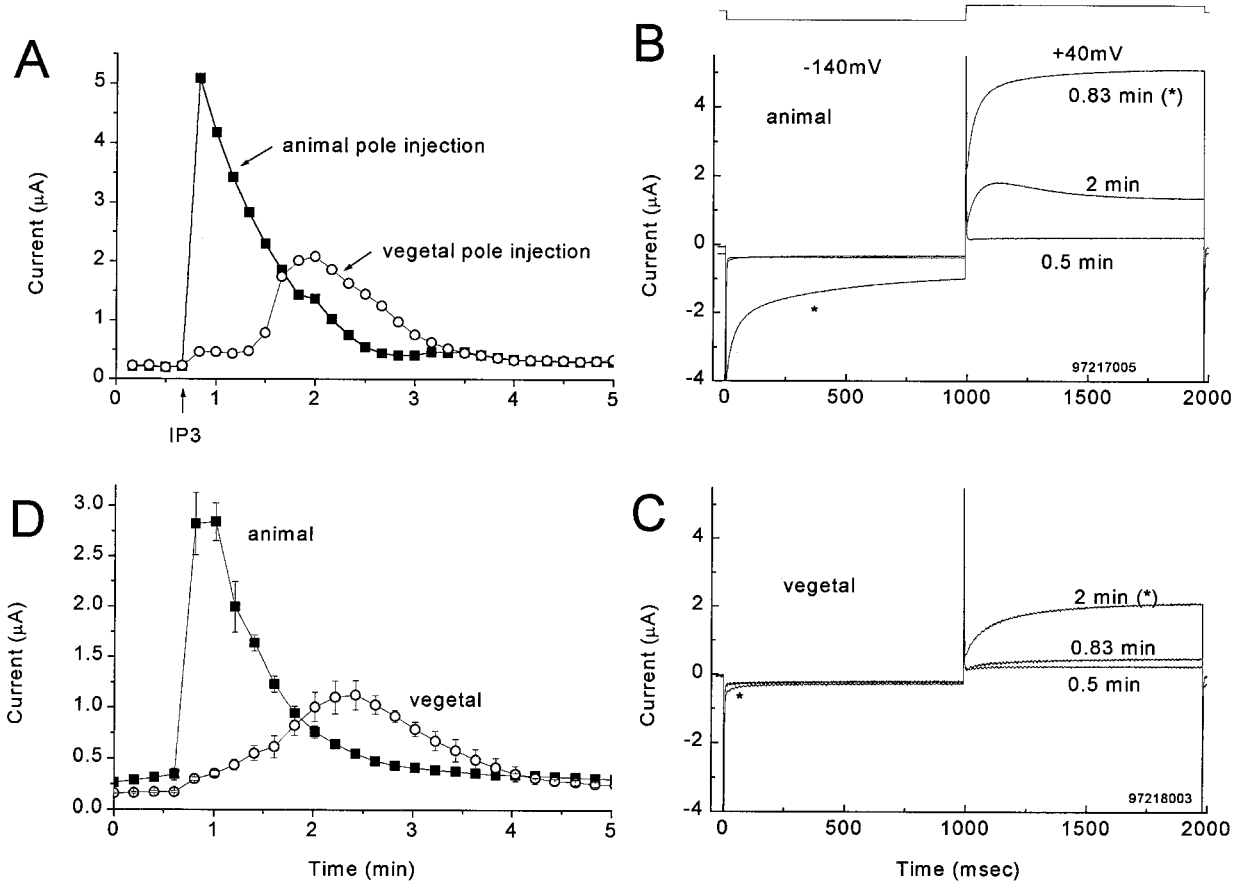

FIGURE 2 Time course of development of $I_{Cl\text{-}1}$ after injection of IP3 into animal or vegetal hemispheres. Oocytes were bathed in normal [Cl] and voltage clamped with a 1-s pulse to -140 mV, followed by a 1-s pulse to $+40$ mV from a holding potential of -35 mV. Stimulation was applied once every 10 s. Twenty-three nanoliters 1 mM IP3 was injected after the fourth stimulation. (*A*) Typical plot of the amplitude of $I_{Cl\text{-}1}$ measured as the current at the end of the $+40$-mV pulse. ■, Animal pole IP_3 injection. ○, Vegetal pole IP_3 injection. (*B*) Current traces corresponding to squares in *A* (animal pole IP_3 injection). Times refer to the times on the *x* axis in *A*. The asterisk identifies the trace at 0.83 min. (*C*) Current traces corresponding to circles in *A* (vegetal pole IP_3 injection). The asterisk identifies the trace at 2 min. (*D*) Average time course of effect of IP_3 injection into 10 oocytes injected in the animal pole (■) and 10 oocytes injected in the vegetal pole (○).

quickly but then plateaued. This was followed by a larger increase that began ~1 min after IP_3 injection. The maximum stimulation of I_{Cl-1} was only to ~2 μA. The time course of activation of I_{Cl-1} upon depolarization to +40 mV was faster when IP_3 was injected into the animal pole versus the vegetal pole (Fig. 2, *B* and *C*). Virtually identical results were obtained in every oocyte tested (Fig. 2 *D*; $n = 10$ for each hemisphere). The observation that injection of IP_3 into the animal hemisphere produced a larger response than injection into the vegetal hemisphere confirms previous results of other investigators (Berridge, 1988; Lupu-Meiri et al., 1988; Parekh, 1995). The larger response upon injection of IP_3 into the animal hemisphere could be explained by differences in density of IP_3 receptors, density of Ca stores, or distribution of Cl channels in the two hemispheres. To distinguish between these possibilities, we performed the same experiment in oocytes that were loaded with Ca-sensitive dyes, so that we could visualize the Ca signal upon IP_3 injection.

In these experiments, oocytes were mounted on the inverted confocal microscope stage such that the confocal section was taken <30 μm from the bottom of the oocyte surface into the vegetal (Fig. 3 *A*) or animal (Fig. 3 *B*) hemispheres. The IP_3 injection pipette was inserted superficially into the opposite pole of the oocyte (Fig. 3, *insets*). Under these conditions, we observed two patterns of re-

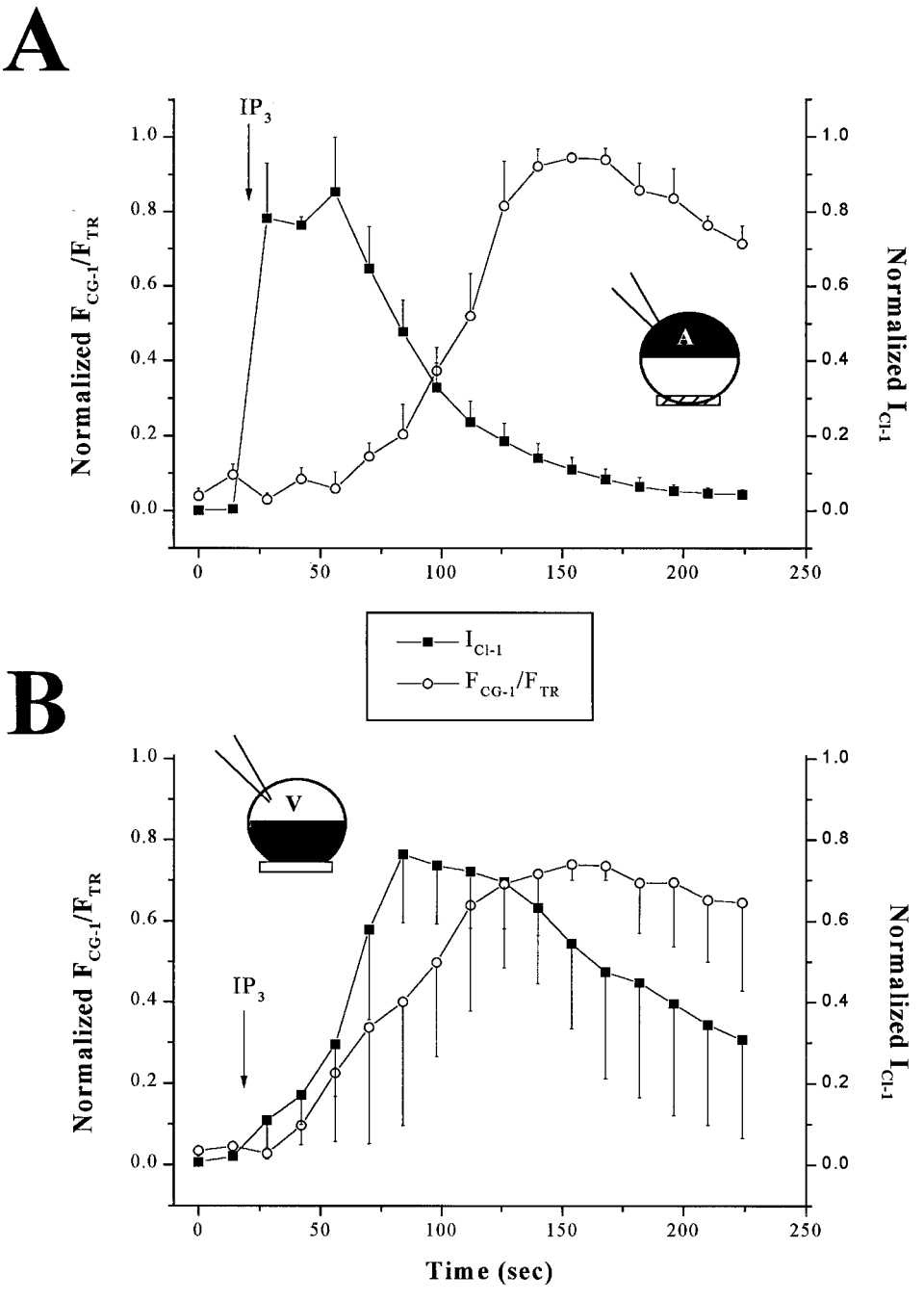

FIGURE 3 Correspondence between I_{Cl-1} and Ca signals at the animal and vegetal poles measured by confocal microscopy. Oocytes were injected with 70 kDa dextran coupled to Ca-Green-1 and Texas Red and were voltage clamped with two microelectrodes. Oocytes were voltage clamped from a holding potential of −35 mV to +40 mV for 2 s and then to −140 mV for 2 s (Hartzell, 1996). The ratio of the Ca-Creen-1 (CG-1) and Texas Red (TR) fluorescence intensities was computed for the entire confocal section near the membrane (F_{CG-1}/FTR) during the pulse to +40 mV (○). I_{Cl-1} was measured as the maximum outward current at +40 mV (■). (*A*) IP_3 was injected into the animal hemisphere after the second pulse, as indicated by the arrow. The confocal image plane was in the vegetal hemisphere and is indicated by the hatched box. The data represent the average ± SE of four cells. (*B*) IP_3 was injected into the vegetal pole after the second pulse, as indicated by the arrow. The confocal image plane was in the animal hemisphere and is indicated by the open box. The variability in the Ca fluorescence appears larger in this case because the signal was much smaller than in the opposite orientation (*A*), because of the pigmentation in the animal pole. I_{Cl-1} currents also appear more variable because currents obtained after IP3 injection in the vegetal pole were smaller than those obtained after IP_3 injection in the vegetal pole (see Fig. 2). The data represent the average ± SE of four cells.

sponses, depending on the site of IP_3 injection (Fig. 2). IP_3 injection into the animal pole (Fig. 2 *A*) produced an immediate (10-s) increase in $I_{Cl\text{-}1}$ (*closed squares*) that peaked in <30 s. The Ca signal (*open circles*), measured in the vegetal hemisphere, did not begin to increase until nearly 1 min later and did not peak until 1.5 min after $I_{Cl\text{-}1}$ had reached its peak. Oocytes oriented in the opposite fashion (Fig. 3 *B*), with IP_3 injected into the vegetal hemisphere and the confocal image taken from the animal hemisphere, produced a different pattern. The time course of increase in the Ca signal was nearly the same as it was when the animal hemisphere was injected, but now $I_{Cl\text{-}1}$ developed much more slowly. The time course of development of $I_{Cl\text{-}1}$ corresponded much more closely with the time course of the Ca signal. One explanation of these results is that the $I_{Cl\text{-}1}$ channels are localized to the animal hemisphere of the oocyte such that the Ca signal and Cl current correspond in time only when the oocyte is oriented such that the confocal image plane passes through the hemisphere that contains the Cl channels.

Effects of Cl-free solution on activation of $I_{Cl\text{-}1}$ by Ca released from stores

To directly determine the distribution of $I_{Cl\text{-}1}$ channels in the oocyte, the oocyte was placed in a chamber in which the animal and vegetal hemispheres of the oocyte could be superfused with different solutions (Experimental Procedures, Fig. 1). Because $I_{Cl\text{-}1}$ is an outward current (inward movement of Cl ions), removal of Cl ions from the extracellular solution should abolish $I_{Cl\text{-}1}$ at positive potentials. In the experiment of Fig. 4, we voltage-clamped the oocyte from a −35-mV holding potential with a 1-s pulse to −140 mV, followed by a 1-s pulse to +40 mV. As we have previously demonstrated under these conditions, $I_{Cl\text{-}1}$ was first activated in response to Ca release from stores as a noninactivating outward current at +40 mV (Fig. 4 *A, trace b, crosses*). After capacitative Ca influx developed, $I_{Cl\text{-}1}$ at +40 mV was activated only transiently because the activation depended upon Ca that had entered the cell during the previous −140 mV pulse (Fig. 4 *A, trace c, triangles*)

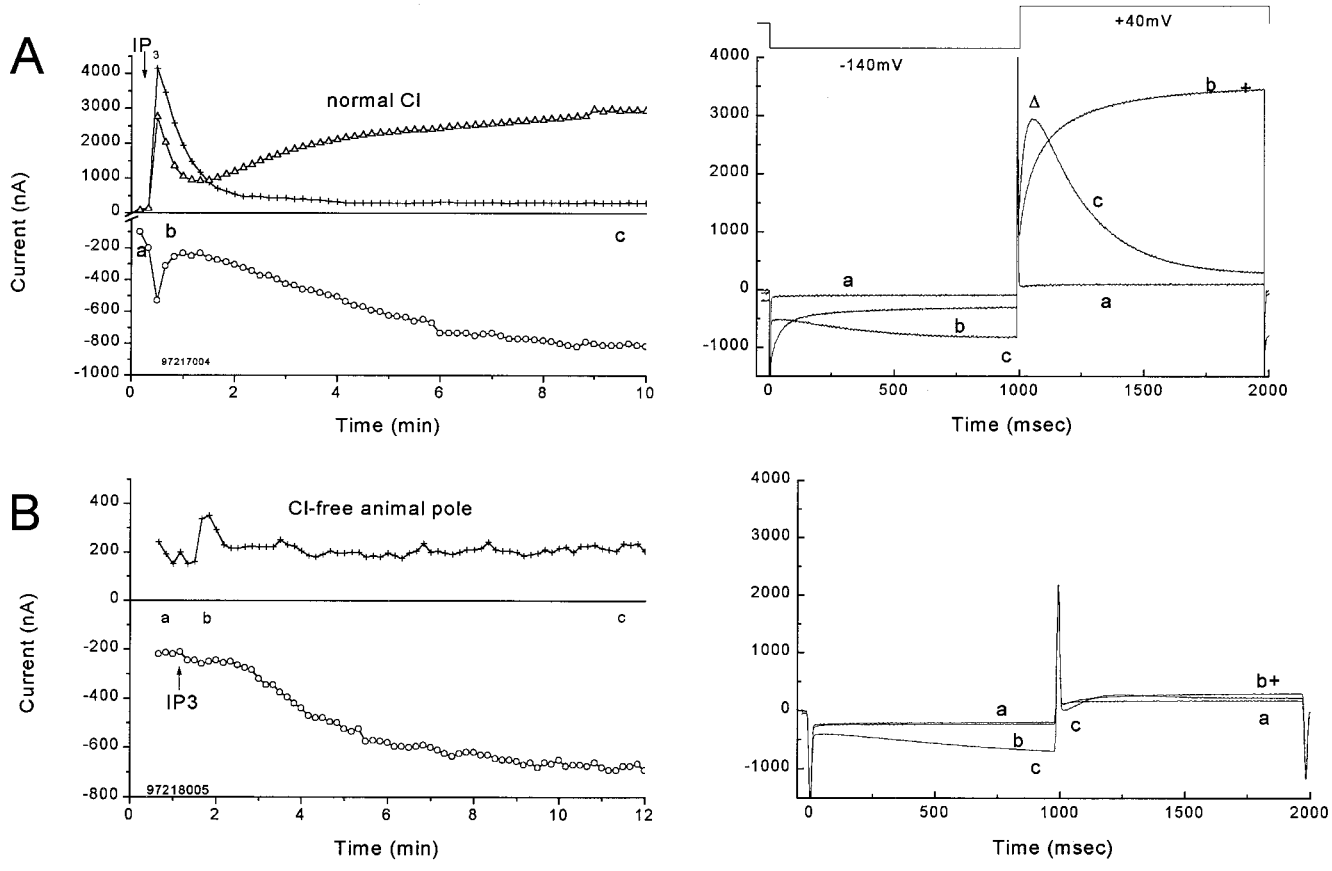

FIGURE 4 Effects of IP_3 injection on $I_{Cl\text{-}1}$ and $I_{Cl\text{-}2}$ in different [Cl] at the animal pole. The oocyte was placed in the two-sided chamber in Fig. 1 and voltage clamped by a 1-s pulse to −140 mV followed by a 1-s pulse to +40 mV from a holding potential of −35 mV. The animal pole was upward. The stimulation was applied once every 10 s. Forty-six nanoliters of 1 mM IP_3 was injected at the arrows. The plots on the left show the time course of development of $I_{Cl\text{-}1}$ and $I_{Cl\text{-}2}$. ○, $I_{Cl\text{-}2}$ measured as the current at the end of the −140-mV pulse. +, $I_{Cl\text{-}1}$ activated by Ca release from stores measured at the end of the +40-mV pulse. △, $I_{Cl\text{-}1}$ transiently activated by Ca influx measured 90 ms after the onset of the +40-mV pulse. The currents on the right correspond to the time points labeled a, b, c in the plot. (*A*) Normal [Cl] at both animal and vegetal poles. (*B*) Cl-free solution at the animal pole and normal [Cl] at the vegetal pole.

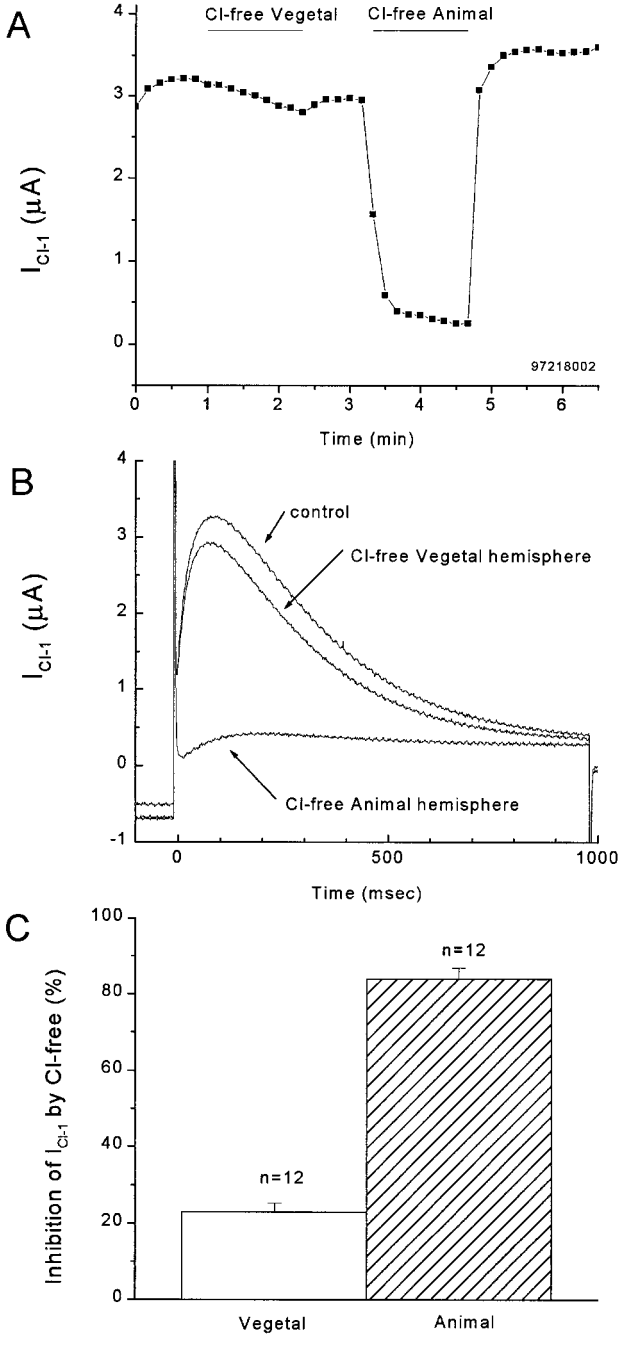

FIGURE 5 Effect of changing extracellular Cl on I_{Cl-1} activated by Ca influx more than 10 min after IP_3 injection. The solution was changed to zero Cl at the animal and vegetal hemisphere of the same oocyte as indicated. (*A*) Plot of peak I_{Cl-1} amplitude (measured 80 ms after onset of +40-mV pulse). (*B*) Current traces corresponding to experiment in *A*. (*C*) Summary of the effects of Cl-free solution applied to the animal and vegetal hemispheres on I_{Cl-1}. Six oocytes were oriented with the animal pole upward and six with the vegetal pole upward. Cl-free solution was tested on both sides of each oocyte. The mean percentage inhibition of I_{Cl-1} (± SE) was plotted. I_{Cl-1} was taken as the peak current at +40 mV after a −140-mV pulse.

(Hartzell, 1996). Fig. 4 *A* shows the control condition where the oocyte was superfused on both sides with normal Cl-containing solution. Injection of IP_3 stimulated I_{Cl-1} that activated rapidly upon depolarization to +40 mV and did not inactivate (Fig. 4 *A, trace b*). This current, which was due to Ca released from internal stores, declined back to baseline in several minutes as the stores became depleted of Ca. In contrast, when the animal hemisphere was superfused with Cl-free solution (Fig. 4 *B, cross, trace b*), I_{Cl-1} was not significantly activated in response to release of Ca from internal stores or to Ca influx. However, I_{Cl-2} was activated normally after ~10 min (compare *circles, trace c* in Fig. 4 *A* and *B*) as capacitative Ca entry developed in response to store depletion. This activation of I_{Cl-2} confirmed that the IP_3 injection had caused release of Ca from internal stores. These data suggested that I_{Cl-1} was activated almost exclusively in the animal pole.

Effects of Cl-free solutions on I_{Cl-1} activated by Ca influx

Although the experiment of Fig. 4 suggested that I_{Cl-1} channels were activated preferentially in the animal pole, the experiment was somewhat unsatisfying, because it was necessary to compare the responses of I_{Cl-1} in different oocytes bathed in normal or Cl-free solution because I_{Cl-1} changed so rapidly with time after IP_3 injection. For this reason, we examined the activation of I_{Cl-1} channels in response to capacitative Ca entry. In Fig. 5, an oocyte was injected with IP_3, and capacitative Ca entry was allowed to develop fully (>10 min), so that I_{Cl-1} was activated transiently at +40 mV after a prepulse to −140 mV to drive Ca entry. The amplitude of I_{Cl-1} in response to a +40-mV depolarization immediately after Ca influx driven by a −140-mV pulse was measured. When the chamber bathing the vegetal hemisphere was changed to Cl-free solution, I_{Cl-1} decreased by ~10–15%. In contrast, when the chamber bathing the animal hemisphere was changed to Cl-free solution, I_{Cl-1} was almost completely abolished. Fig. 5 *C* shows the average percentage inhibition of I_{Cl-1} when the Cl-free solution was placed on the animal or vegetal hemisphere. Six of the oocytes were oriented with the animal hemisphere upward and six with the vegetal hemisphere upward, and Cl-free solution was tested on both vegetal and animal hemispheres in every oocyte. These data suggest that the density of I_{Cl-1} was four times higher in the animal than in the vegetal pole.

This preferential activation could most easily be explained if the I_{Cl-1} channels were localized to the animal pole. However, an alternative possibility is that both Ca stores and capacitative Ca entry are localized to the animal pole and that Cl channels are uniformly distributed to both animal and vegetal hemispheres. This possibility is unlikely, considering the results of Fig. 3, but the following experiments tested this more rigorously.

Spatial localization of Ca release and capacitative Ca entry

To answer the question of whether Ca influx and release were localized to one or the other pole, the oocyte was

oriented with either the animal or vegetal pole facing upward, with the confocal section passing through the opposite hemisphere. IP_3 was injected into the hemisphere facing up (Fig. 6, *insets*), and we compared the Ca signal in the animal and vegetal hemispheres.

To compare Ca influx and Ca release in the two poles, we reasoned that we could separate influx and release by stepping the membrane between +40 mV, where the driving force for Ca influx would be very low, and −140 mV, where the driving force for Ca influx would be high (Hartzell, 1996). Thus the difference in the Ca signal at −140 mV and +40 mV was used as an indication of Ca influx. This signal was completely obliterated by the removal of extracellular Ca (Machaca and Hartzell, manuscript in preparation). This signal is likely to be an overestimate of the actual influx, because capacitative Ca influx is known to trigger Ca release from stores through a Ca-activated Ca release mechanism in *Xenopus* oocytes (Yao and Parker, 1993, 1994; Girard and Clapham, 1993). Such Ca release from stores could contaminate our influx fluorescence signal. However, because we inject supramaximum levels of IP_3, we expect that the stores are largely Ca-depleted. In fact, subsequent IP_3 injections tens of minutes after the initial injection do not induce any additional Ca release from stores, but this could be due to inactivation of the IP_3 receptor. Nevertheless, because release of Ca from stores is voltage-independent (Machaca and Hartzell, manuscript in preparation), we believe that the difference between the

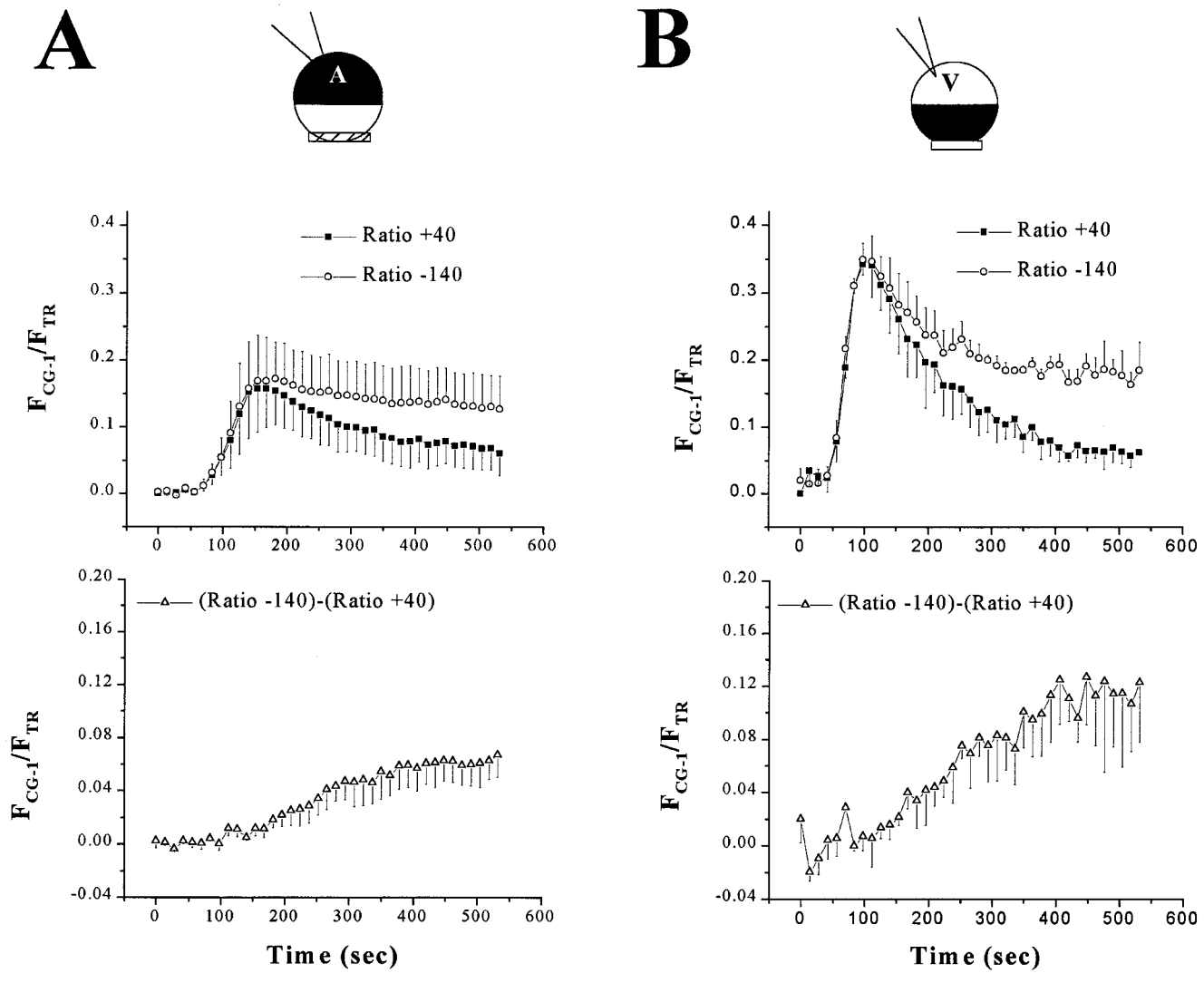

FIGURE 6 Ca release and influx in animal and vegetal poles. The experimental setup was similar to that in Fig. 3, with IP_3 injected after the second pulse. The average ratios of Ca-Green-1 (CG-1) and Texas Red (TR) fluorescence at +40 mV (■) and at −140 mV (○) in the confocal section of the vegetal (*A*) or animal (*B*) hemispheres are plotted ± SE. Insets represent the orientation of the oocyte and the hemisphere of IP_3 injection and confocal imaging. The difference between the Ca signals at −140 mV and +40 mV is plotted in the lower panels (△). This difference signal is a measure of the voltage-dependent Ca influx. The data are the average of four to six cells. Ca release in the animal pole as calculated from the fluorescence ratio at +40 was almost double that of release in the vegetal pole (Release animal/Release vegetal = 1.95). Ca influx in the animal pole was also almost double that in the vegetal pole (Influx animal/Influx vegetal = 1.88)

+40-mV and −140-mV Ca signals provides a reasonable assessment of Ca influx-dependent cytosolic Ca. Injection of IP_3 into either pole caused an increase in the fluorescence ratio at both +40 mV and −140 mV in both the vegetal (Fig. 6 *A*) and animal (Fig. 6 *B*) hemispheres because of Ca release from stores. The increase in fluorescence ratio in the animal hemisphere was almost double (1.95×) that in the vegetal hemisphere (as one might expect from the lower density of IP_3R in the vegetal hemisphere; Callamaras and Parker, 1994). The Ca influx-dependent signal in the animal hemisphere, estimated by the difference between the −140 mV and +40 mV Ca signals, was almost double (1.88×) that in the vegetal hemisphere (Fig. 6, *A* and *B*, *lower panels*). These data show that there is significant Ca release and capacitative Ca entry in both the animal and vegetal poles. However, the levels of Ca release and influx are twofold higher in the animal hemisphere. This twofold difference could partly account for the differences in $I_{Cl\text{-}1}$ amplitude in response to IP_3 injection in the two hemispheres, but is unlikely to explain the almost complete absence of $I_{Cl\text{-}1}$ current when the animal pole is bathed in Cl-free solution.

Distribution of $I_{Cl\text{-}2}$ channels in the oocyte

These data show that capacitative Ca entry occurs over the entire surface of the oocyte, but that $I_{Cl\text{-}1}$ channels are primarily localized to the animal hemisphere. Knowing that store-operated Ca channels are present in both animal and vegetal hemispheres, we were now able to evaluate the distribution of $I_{Cl\text{-}2}$ channels. These experiments are illustrated in Fig. 7. In these experiments, we recorded the amplitude of oocyte Cl currents with a large (40-μm inside diameter) extracellular patch pipette as described in the Experimental Procedures. First, to establish the spatial resolution of the extracellular recording, we made a patch on the animal pole of the oocyte after capacitative Ca entry and

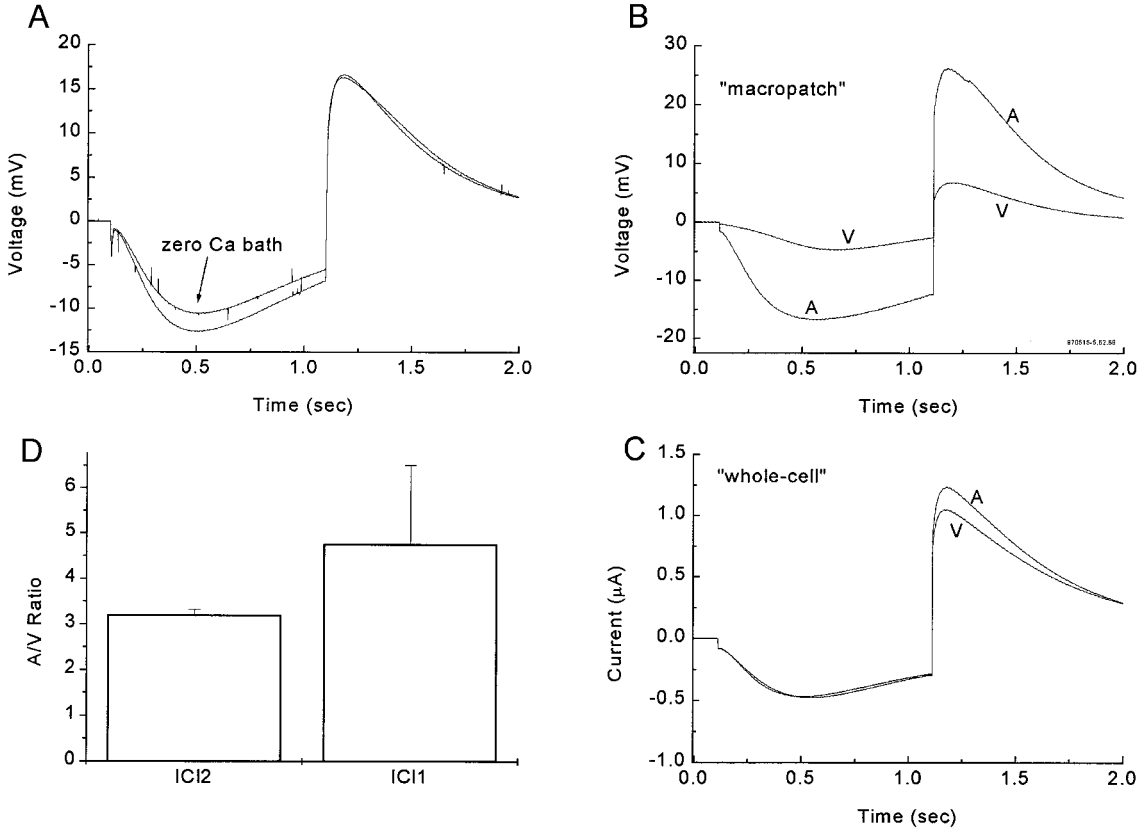

FIGURE 7 Distribution of $I_{Cl\text{-}2}$ channels. Oocytes were voltage-clamped with two microelectrodes and stimulated by 1-s pulses to −140 mV and +40 mV as described above. In addition, a ~40-μm-diameter patch pipette was placed on the surface of the animal or vegetal hemisphere of the oocyte as indicated, and the voltage at the surface of the oocyte was measured. (*A*) Demonstration that the patch pipette localizes the currents to the region under the pipette. Two traces from the macropatch pipette are superimposed: one with normal Ca in both the bath and the pipette, and one with zero Ca in the bath and normal Ca in the patch pipette. (*B*) Recordings from the macropatch pipette when it was positioned on the center of the animal (A) or vegetal (V) pole while the potential of the oocyte was changed by the two-microelectrode voltage clamp. (*C*) Whole-cell currents recorded by the two-microelectrode voltage clamp when the macropatch pipette was positioned on the animal (A) or vegetal (V) pole. The traces were recorded simultaneously with the macropatch recordings in *B*. (*D*) Summary of four experiments like that shown in *B* and *C*. The ratio of amplitude of the responses recorded at the animal (A) and vegetal (V) hemispheres for each oocyte was calculated. $I_{Cl\text{-}1}$ was taken as the peak current at +40 mV and $I_{Cl\text{-}2}$ was taken as the maximum current at −140 mV.

$I_{Cl\text{-}2}$ had developed fully in response to IP_3 injection. The bath solution was then changed to zero Ca solution to eliminate Ca influx from regions outside the patch pipette (Fig. 7 *A*). Elimination of bath Ca had very little effect on the amplitude of the currents measured by the patch pipette, showing that the macropatch pipette was effective in recording only the channels lying under the pipette. To determine the distribution of $I_{Cl\text{-}1}$ and $I_{Cl\text{-}2}$ channels in the oocyte, the macropatch pipette was positioned on opposite poles of the same oocyte. The currents recorded by the macropatch pipette were markedly different when it was positioned on the different poles: both $I_{Cl\text{-}1}$ and $I_{Cl\text{-}2}$ were smaller when the macropatch pipette was on the vegetal pole (Fig. 7 *B*). Fig. 7 *C* shows that the currents recorded from the whole cell (by the simultaneous two-microelectrode voltage-clamp recording) did not change appreciably during the time required to reposition the micropatch pipette. Fig. 7 *D* shows the average ratio of the amplitude of the Cl currents recorded from animal and vegetal poles of four oocytes tested in this way. These data suggest that the density of $I_{Cl\text{-}1}$ was 4.7 times higher in the animal than in the vegetal hemisphere, which confirmed the data presented in Fig. 5 *C*, whereas the density of $I_{Cl\text{-}2}$ was 3.2 times higher in the animal hemisphere. Thus it appears that $I_{Cl\text{-}1}$ may be somewhat more highly localized spatially than is $I_{Cl\text{-}2}$.

DISCUSSION

In this study we have shown that $I_{Cl\text{-}1}$ channels are asymmetrically distributed in *Xenopus* oocytes by four different kinds of measurements. First, the kinetics of increase in $I_{Cl\text{-}1}$ were slower when IP_3 was injected into the vegetal hemisphere than when it was injected into the animal hemisphere. Second, $I_{Cl\text{-}1}$ amplitude depended on extracellular Cl at the animal hemisphere, regardless of whether $I_{Cl\text{-}1}$ was activated by Ca released from internal stores or by Ca influx. Third, the increase in $I_{Cl\text{-}1}$ coincided with the appearance of the wave of Ca release at the animal hemisphere by confocal microscopy of oocytes loaded with Ca-sensitive dyes. Fourth, extracellular recording showed that $I_{Cl\text{-}1}$ current density was much higher in the animal pole. We conclude that the density of $I_{Cl\text{-}1}$ current in the animal pole is about four or five times higher than it is in the vegetal pole. We also find that $I_{Cl\text{-}2}$ current is localized to the animal pole, although the difference in density between the animal and vegetal poles is somewhat less, about threefold. The difference in density of the currents in the two poles could be due partly to differences in the amplitude of the Ca signal in the two hemispheres. We find that the levels of Ca release and Ca entry in the animal hemisphere are about twofold higher in the animal versus the vegetal hemispheres (Fig. 6), which could account, at least in part, for the five- and threefold differences observed for $I_{Cl\text{-}1}$ and $I_{Cl\text{-}2}$. However, we favor the idea that the difference in current density reflects differences in the density of the Cl channels in the two hemispheres because of the arguments presented below.

Several investigators have previously shown that Ca-activated Cl current responses are asymmetrically distributed in *Xenopus* oocytes (Berridge, 1988; Robinson, 1979; Lupu-Meiri et al., 1988; Parekh, 1995). Lupu-Meiri et al. (1988) showed that injection of IP_3 into the animal hemisphere produced larger and slower inward currents than when it was injected into the vegetal hemisphere. However, injections of $CaCl_2$ into animal and vegetal hemispheres produced responses of similar amplitude but slower kinetics in the vegetal hemisphere. In contrast, Miledi and Parker (1984) reported a ~13-fold larger Cl current level after Ca injection in the animal versus the vegetal hemisphere, and Gomez-Hernandez et al. (1997) showed that Ca-activated Cl current is ~10-fold enriched in the animal pole in inside-out macropatches. The differences between the Ca injection studies of Lupu-Meiri et al. and Miledi and Parker could be reconciled by the fact that Miledi and Parker injected ~400-fold less Ca (~0.5 pmol) than Lupu-Meiri et al. (~200 pmol). Injection of large amounts of Ca into the vegetal pole could result in fast diffusion of Ca or Ca-induced Ca release and activation of Cl channels in the animal hemisphere. This explanation is especially plausible because Lupu-Meiri et al. (1988) observed a ~25-s time lag to reach maximum current amplitude after vegetal pole versus animal pole Ca injections. The ~13-fold larger Cl current after Ca injection observed by Parker and Miledi and the ~10-fold enrichment of Cl currents in inside-out patches from the animal pole (Gomez-Hernandez et al., 1997) support our conclusion that the difference in Cl current levels is due to preferential localization of the $I_{Cl\text{-}1}$ channels to the animal hemisphere.

The localization of endogenous ion channels to the animal pole is not unexpected. The *Xenopus* oocyte is a distinctly polarized cell with the nucleus located in the center of the animal pole. There are marked morphological differences between the two hemispheres (Brachet, 1977; Nieuwkoop, 1977), and exogenously expressed receptors and ion channels are often clustered at one hemisphere (Robinson, 1979; Peter et al., 1991; Parekh, 1995). The mechanisms responsible for generating and maintaining the polarized nature of expression of exogenous ion channels has been discussed in detail by Peter et al. (1991). These investigators suggest that there is a directed transport process that involves microtubules and actin cytoskeleton, because cytoskeletal-disupting drugs result in a randomization of the distribution of expressed ion channels.

Our results are significant because they provide additional information about spatial features of the Ca signaling pathways in *Xenopus* oocytes. *Xenopus* oocytes are a popular model system for studying Ca signaling, and the question of how Ca released from stores and Ca influx can differentially regulate two different Cl channels is an important one. These results indicate that the spatial distribution of Cl channels may have an impact on the way in which Ca signals are decoded by them. However, at the present time we do not have sufficient information to propose a

model of how the two currents are regulated by Ca released from stores and by Ca influx.

An obvious question that is raised by these studies involves the physiological role of these Ca-activated Cl channels. It is well known that fertilization results in a Ca transient that can activate these channels (see references in Busa et al., 1985). The Ca transient triggers cortical granule exocytosis and block to polyspermy, but the role of the Cl currents is not clearly defined. The activation of Cl currents could play a role in promoting HCO_3 or water flux to regulate intracellular pH or osmotic balance subsequent to fertilization. Alternatively, activation of Cl channels could also play other as yet undefined developmental roles (Moody et al., 1991).

We thank Lynne Quarmby and Harish Joshi for helpful discussions.

REFERENCES

Berridge, M. J. 1988. Inositol triphosphate-induced membrane potential oscillations in *Xenopus* oocytes. *J. Physiol. (Lond.).* 403:589–599.

Berridge, M. J. 1995. Capacitative calcium entry. *Biochem. J.* 312:1–11.

Brachet, J. 1977. An old enigma: the gray crescent of amphibian eggs. *Curr. Top. Dev. Biol.* 11:133–186.

Busa, W. B., J. E. Ferguson, S. K. Joseph, J. R. Williamson, and R. Nuccitelli. 1985. Activation of frog (*Xenopus laevis*) eggs by inositol trisphosphate. *J. Cell Biol.* 101:677–682.

Callamaras, N., and I. Parker. 1994. Inositol 1,4,5-trisphosphate receptors in *Xenopus laevis* oocytes: localization and modulation by Ca^{2+}. *Cell Calcium.* 15:66–78.

Camacho, P., and J. D. Lechleiter. 1995. Calreticulin inhibits intracellular Ca^{2+} waves. *Cell.* 82:765–771.

Clapham, D. 1995. Calcium signaling. *Cell.* 80:259–268.

Dascal, N. 1987. The use of *Xenopus* oocytes for the study of ion channels. *CRC Crit. Rev. Biochem.* 22:317–387.

Delisle, S. 1991. The four dimensions of calcium signalling in *Xenopus* oocytes. *Cell Calcium.* 12:217–227.

Delisle, S., and M. Welsh. 1992. Inositol trisphosphate is required for the propagation of calcium waves in *Xenopus* oocytes. *J. Biol. Chem.* 267:7963–7966.

Fasolato, C., B. Innocenti, and T. Pozzan. 1994. Receptor-activated Ca^{2+} influx: how many mechanisms for how many channels? *Trends Pharmacol. Sci.* 15:77–83.

Ghosh, A., and M. E. Greenberg. 1995. Calcium signaling in neurons: molecular mechanisms and cellular consequences. *Science.* 268: 239–247.

Girard, S., and D. Clapham. 1993. Acceleration of intracellular calcium waves in *Xenopus* oocytes by calcium influx. *Science.* 260:229–232.

Gomez-Hernandez, J.-M., W. Stuhmer, and A. B. Parekh. 1997. Calcium dependence and distribution of calcium-activated chloride channels in *Xenopus* oocytes. *J. Physiol. (Lond.).* 502.3:569–574.

Hartzell, H. C. 1996. Activation of different Cl currents in *Xenopus* oocytes by Ca liberated from stores and by capacitative Ca influx. *J. Gen. Physiol.* 108:157–175.

Hartzell, H. C., K. Machaca, and Y. Hirayama. 1997. Effects of adenophostin-A and IP_3 on Cl currents in *Xenopus* oocytes. *Mol. Pharmacol.* 51:683–692.

Lechleiter, J. D., and D. E. Clapham. 1992. Molecular mechanisms of intracellular calcium excitability in *X. laevis* oocytes. *Cell.* 69:283–294.

Lenzi, D., and W. M. Roberts. 1994. Calcium signalling in hair cells: multiple roles in a compact cell. *Curr. Opin. Neurobiol.* 4:496–502.

Lupu-Meiri, M., H. Shapira, and Y. Oron. 1988. Hemispheric asymmetry of rapid chloride responses to inositol trisphosphate and calcium in *Xenopus* oocytes. *FEBS Lett.* 240:83–87.

Miledi, R., and J. Parker. 1984. Chloride current induced by injection of calcium into *Xenopus* oocytes. *J. Physiol. (Lond.).* 357:173–183.

Moody, W. J., L. Simoncini, J. L. Coombs, A. E. Spruce, and M. Villaz. 1991. Development of ion channels in early embryos. *J. Neurobiol.* 22:674–684.

Nieuwkoop, P. D. 1977. Origin and establishment of embryonic polar axes in amphibian development. *Curr. Top. Dev. Biol.* 11:115–132.

Parekh, A. B. 1995. Interaction between capacitative Ca^{2+} influx and Ca^{2+}-dependent Cl^- currents in *Xenopus* oocytes. *Pflugers Arch.* 430: 954–963.

Parker, I., J. Choi, and Y. Yao. 1996. Elementary events of $InsP_3$-induced Ca^{2+} liberation in *Xenopus* oocytes: hot spots, puffs and blips. *Cell Calcium.* 20:105–121.

Parker, I., and R. Miledi. 1987. Inositol trisphosphate activates a voltage-dependent calcium influx in *Xenopus* oocytes. *Proc. R. Soc. Lond.* 231:27–36.

Parker, I., and Y. Yao. 1994. Relation between intracellular Ca^{2+} signals and Ca^{2+}-activated Cl^- current in *Xenopus* oocytes. *Cell Calcium.* 15:276–288.

Peter, A. B., J. C. Schittny, V. Niggli, H. Reuter, and E. Sigel. 1991. The polarized distribution of poly(A^+)-mRNA-induced functional ion channels in the *Xenopus* oocyte plasma membrane is prevented by anticytoskeletal drugs. *J. Cell Biol.* 114:455–464.

Putney, J. W. 1990. Capacitative calcium entry revisited. *Cell Calcium.* 11:611–624.

Quarmby, L. M., and H. C. Hartzell. 1994. Dissection of eukaryotic transmembrane signalling using *Chlamydomonas. Trends Pharmacol. Sci.* 15:343–349.

Robinson, K. R. 1979. Electrical currents through full-grown and maturing *Xenopus* oocytes. *Proc. Natl. Acad. Sci. USA.* 76:837–841.

Thomas, A. P., G. St. J. Bird, G. Hajnoczky, L. D. Robb-Gaspars, and J. W. Putney, Jr. 1996. Spatial and temporal aspects of cellular calcium signaling. *FASEB. J.* 10:1505–1512.

Yao, Y., and I. Parker. 1993. Inositol trisphosphate-mediated Ca^{2+} influx into *Xenopus* oocytes triggers Ca^{2+} liberation from intracellular stores. *J. Physiol. (Lond.).* 468:275–296.

Yao, Y., and I. Parker. 1994. Ca^{2+} influx modulation of temporal and spatial patterns of inositol trisphosphate-mediated Ca^{2+} liberation in *Xenopus* oocytes. *J. Physiol. (Lond.).* 476:17–28.